



Contents lists available at ScienceDirect

Current Research in Microbial Sciences

journal homepage: www.sciencedirect.com/journal/current-research-in-microbial-sciences

Relevance of iron metabolic genes in biofilm and infection in uropathogenic *Proteus mirabilis*

V Iribarnegaray^{a,d}, MJ González^b, AL Caetano^a, R Platero^c, P Zunino^a, P Scavone^{b,*}

^a Department of Microbiology, Instituto de Investigaciones Biológicas Clemente Estable, Avda. Italia 3318, Montevideo CP 11600, Uruguay

^b Laboratory of Microbial Biofilms, Department of Microbiology, Instituto de Investigaciones Biológicas Clemente Estable, Avda. Italia 3318, Montevideo CP 11600, Uruguay

^c Department of Biochemistry and Microbial Genomics, Instituto de Investigaciones Biológicas Clemente Estable, Avda. Italia 3318, Montevideo CP 11600, Uruguay

^d Department of Pathobiology, Facultad de Veterinaria, Universidad de la República, Alberto Lasplacas 1620, Montevideo, Uruguay

ARTICLE INFO

Keywords:

Proteus mirabilis
 biofilms
 Urinary tract infection
 Iron
 Non-heme ferritin
 Ton-B receptor

ABSTRACT

The microorganisms are found in the environment, forming sessile communities embedded in an extracellular matrix of their own production, called biofilm. These communities have a great relevance in the clinical context, since they are associated with infections caused by biofilm in medical implants, such as urinary catheters. The development of biofilms is a complex process where a great diversity of genes participate. The present work is based on the study of genes related to iron metabolism and its implication in the development of *P. mirabilis* biofilms and pathogenicity. For this study, two mutant strains defective in biofilm formation were selected, generated by the interruption of genes that encoded non-heme ferritin and TonB-dependent receptor. The mutations influence on the development of the biofilm was evaluated by different approaches. The complexity of the biofilm was analyzed using Confocal Laser Microscopy and image analysis. The mutants infectivity potential was assessed in two experimental mice models of urinary tract infection. The results obtained in the present work show us the role of the ferritin and a TonB-associated porin protein over the initial and later stages of biofilm development. Moreover, in the ascending UTI mouse model, both mutants failed to colonize the urinary tract. In CAUTI models, ferritin mutant damaged the bladder similarly to wild type but the Ton-B mutant was unable to generate infection in the urinary tract. The results obtained in the present work confirm the relevant role that iron metabolism genes have in *P. mirabilis* biofilm development and for infection in the urinary tract.

1. Introduction

Iron is one of the most abundant metals in the earth, although its availability for microorganisms is limited. The host limits iron availability as part of its innate defense against invading cellular microorganisms. Mammals use iron-binding proteins (e.g., transferrin, lactoferrin) to reduce the levels of free extracellular iron to around 10^{-18} M (Bullen et al. 1978), insufficient to allow bacterial growth (Litwin et al. 1993). Many bacteria have developed complex systems to capture iron and regulate its acquisition (Hantke et al. 2001). The importance of this regulation is based on the role of iron in the survival of several bacteria. Iron is necessary for the bacteria metabolism, for example in protein synthesis, generation of energy (Crichton, 2016), and virulence and host colonization. Bacteria express a multitude of complex systems to capture iron, like heme acquisition systems, transferrin or

lactoferrin receptors, ferric or ferrous iron transporters, and production of low molecular weight compounds, called siderophores (Bullen et al., 1999).

The role of iron during infection is well known. Hagan and Mobley (2009), reported that an *Escherichia coli* (UPEC) mutant strain that was deficient for heme utilization, was unable to colonize the murine kidney compared with the wild type. A TonB mutant was severely attenuated *in vivo*, indicating that TonB-dependent systems are required for UPEC colonization (Torres et al., 2001). *Proteus mirabilis* is an important etiologic agent of complicated urinary tract infections (UTI). It is the most commonly found microorganism in long-term catheterization (Wazait et al., 2003; Stickler and Feneley, 2010) and causes approximately 3% of all nosocomial infections and up to 44% of UTI associated to catheterization (CAUTI) in the United States (O'Hara et al., 2000; Jacobsen et al., 2008; Stickler and Feneley, 2010; Stickler, 2014). One of

* Corresponding author.

E-mail address: pscavone@iibce.edu.uy (P. Scavone).

<https://doi.org/10.1016/j.crmicr.2021.100060>

Received 9 March 2021; Received in revised form 19 July 2021; Accepted 15 August 2021

Available online 17 August 2021

2666-5174/© 2021 The Author(s).

Published by Elsevier B.V. This is an open access article under the CC BY-NC-ND license

(<http://creativecommons.org/licenses/by-nc-nd/4.0/>).

the complication of *P. mirabilis* CAUTI is due to the presence of crystalline biofilms inside and outside the catheters. Urease activity is a key factor in this type of biofilms, in *P. mirabilis* it is constitutively expressed in urine (Flores-Mireles et al., 2015). Also, MR/P fimbriae is relevant in the initial steps of biofilms formation, as also other fimbriae like ATF fimbriae (Scavone et al., 2016). Moreover, *P. mirabilis* biofilm evaluated *in vitro* shown a specific pattern of evolution over 7 days (Schlapp et al., 2011).

The objective of the present study was to analyze the contribution of two genes related to iron acquisition system in *P. mirabilis* biofilm formation. The relevance of these genes was substantiated *in vitro* biofilm formation and *in vivo* urinary tract infection models in mice.

2. Material and methods

2.1. Bacterial strains and growth conditions

P. mirabilis Pr2921 (2921-WT) used in this study is a clinical isolate from a patient with symptomatic UTI (Montevideo, Uruguay) that was previously genotypically and phenotypically characterized in our laboratory (Zunino et al., 200020012003; Schlapp et al., 2011; Giorello et al., 2016). Bacteria were routinely cultured in Luria-Bertani broth (LB) or Luria-Bertani agar (LA) and supplemented with kanamycin (50 µg mL⁻¹) and tetracycline (100 µg mL⁻¹) when necessary. Nutrient agar (NA) was also used for plate counting to avoid swarming motility. FeCl₃ (15 µM, Sigma) was employed for iron supplementation and 2,2-dipyridyl (200 µM Sigma) to generate iron-restriction conditions (Tomaras et al., 2003). All solutions were filter sterilized through 0.22 µm pore size filters and stored at 4 °C until use.

2.2. Random transposon mutagenesis and biofilm screening

The pBAM1 suicide vector harbouring a mini-Tn5 Km derivative was introduced into *P. mirabilis* 2921 by bi-parental conjugation from a donor *E. coli* S17λpir (Martinez-Garcia et al. 2011). *P. mirabilis* trans-conjugants were selected in presence of kanamycin (40 µg/ml) and tetracycline (10 µg/ml), and subsequently screened to identify those with defects in biofilm formation using the crystal violet (CV) microtitre plate assay (Pratt and Kolter, 1998). Briefly, mutants were grown in LB broth in 96 well plates in duplicate for 48 h at 37 °C. Following incubation, planktonic cells were removed and biofilm was stained with 1% CV for 15 min, followed by three washes in PBS to remove the dye excess. The remaining CV associated with the biofilm was then solubilized by addition of 95% (v/v) EtOH. Eluates were transferred to new

plates, and the absorbance measured at 595 nm to determine levels of mutant biofilm formation compared to the wild type. Growth of the mutants was also compared with the wild type during these screens, by measuring absorbance at 600 nm. Mutants with CV absorbance readings of ≤ 0.2 but no attenuation in general growth (no difference in LB broth growth measured at OD600nm) were selected as biofilm deficient (BFD) and subject to further study. Mutants generating an OD of > 0.9 in the CV assay (but with no changes in growth as above) were classified as biofilm enhanced (BFE) (Villegas et al., 2013).

2.3. Genetic characterization of transconjugants and identification of disrupted genes

All transconjugants were analyzed by Southern hybridization as previously described to confirm single Tn insertions (Maniatis et al., 1982). To identify the genes disrupted by Tn insertions, chromosomal DNA flanking inserts were amplified by PCR using a 2-step reaction as previously described (Martinez-Garcia et al., 2011). Primers for both rounds are shown in Table 1. PCR products from the first round of amplification using the primer ARB6 in combination with the transposon specific primers ME-I-extR or ME-O-extF, were used as templates for the second-round PCR with primers ARB2 and ME-I- intR or ME-O-intF (Martinez-Garcia et al., 2011). PCR products from the second round were sequenced (Macrogen Inc, Seoul, Korea) and mapped in the *P. mirabilis* HI4320 genome sequence (GenBank accession no. NC_010555) using Blastn search (BLAST; National Center for Biotechnology Information, USA [http://blast.ncbi.nlm.nih.gov/Blast.cgi]) (Ye et al., 2012). Polar effects of the transposon insertions in the selected mutant strains were evaluated using quantitative real time (qRT)-PCR to confirm if expression of downstream gene was uncompromised, as previously described (Holling et al., 2014), under standard culture conditions described above. Primers for these assays were designed using Primer-Blast (Ye et al., 2012) and are provided in Table 1.

2.4. Assessment of motility

Swarming and swimming motility were evaluated as previously described (Jones et al., 2004; Holling et al., 2014). Briefly, to evaluate swarming motility, 10 µl of an overnight culture were inoculated onto the center of each LB agar plate (1.5% agar). The drops were allowed to soak and then the plates were incubated for 10 h at 37 °C. The assay was performed 3 times. To assess swimming motility, 5 µl of a culture with 10⁸ colony-forming units (cfu) were stabbed into the center of LB agar (LB supplemented with 0.3% agar) and the plates were incubated for 5 h

Table 1.
Primers used in this study.

Application	Primers	Sequence (5' to 3')	Reference
Arbitrary PCR	ARB6	GGCACGCGTCGACTAGTACNNNNNNNNNACGCC	Martinez-Garcia et al. (2011)
	ARB2	GGCACGCGTCGACTAGTAC	
	ME-O-extF	CGGTTTACAAGCATAACTAGTGC	
	ME-O-intF	AGAGGATCCCGGGTACCGAGCTCG	
	ME-I-extR	CTCGTTTCACGCTGAATATGGCTC	
	ME-I-intR	CAGTTTATTGTTTCATGATGATATA	
Real Time PCR	Ftn reverse	TCAGCAGGTGGTGCTTCAAT	This work
	Ftn forward	GCGCTTGGTGCGATGATAAA	This work
	tonB reverse	GGTTAGCTCAGCGGTCACCTT	This work
	tonB forward	GCTTGCTAAAAGCCGATCAGC	This work
	rpoA reverse	AAGCCTCGCTCTAATGGCTC	This work
	rpoA forward	GTTTCTAAAACCGGCGCTGG	This work
genomic context 2021–110	PMI-RS18435 forward	CCATCACCCAGCTCATTGGT	This work
	PMI-RS18435 reverse	ATCGCTCATTTCACCCCGTT	This work
	PMI_RS18430 forward	TAAAGAGCAAGGCTCACGCA	This work
	PMI_RS18430 reverse	CGCACCTTGTGATTGGCAC	This work
genomic context 2021–50	PMI_RS04900 forward	TGGTCGCTAACGATATGGCA	This work
	PMI_RS04900 reverse	AAGCATGCAGCACAAGCATC	This work
	PMI_RS04895: forward	TGGTCGCTAACGATATGGCA	This work
	PMI_RS04895: reverse	AAGCATGCAGCACAAGCATC	This work

at 37 °C. Nine independent swimming assays were performed in order to compare the values among the different strains using Student Test. The distances migrated on both agar types of from the point of inoculation were measured.

2.5. Characterization of cellular hydrophobicity

Cellular hydrophobicity was assessed according to Bibiloni and colleagues (Bibiloni et al., 2001). Bacterial suspensions were prepared in PBS from fresh plates at an $OD_{540}=0.2-0.3$. Ten μl of the suspensions were used to inoculate 5 ml of LB, which were incubated at 37 °C for 48 h under static conditions. Then, bacterial suspensions from the 48 h cultures were prepared at an $OD=0.8$ in PBS and 200 μl of xylene was added. Tubes were shaken for 2 min and left static for another 20 min. After that, OD of the aqueous phase was measured at 600 nm. The hydrophobicity index was calculated using the following equation: $(A0-A)/A0 \times 100$. A0 and A were the values obtained before and after xylene extraction, respectively. Three independent assays were used in order to compare the values of hydrophobicity index among the strains.

2.6. Migration across urinary catheters

The mutants' ability to migrate across urethral catheters, was evaluated as previously described (Stückler and Hughes, 1999). Plates containing 12 ml of LB Agar were dried at ambient temperature for 3 h and then a 1 cm channel was cut along the centerline of the plate. A second perpendicular channel intersecting the first one was cut, isolating a third of the agar and generating four isolated agar blocks. The larger agar blocks were used to evaluate migration over catheters while the two smaller agar blocks served as in plate controls. Two 10 μl aliquots of 4 h culture were inoculated at the edge of the central channel on one of the larger agar blocks, and one 10 μl aliquot was inoculated onto the corresponding small agar block. Once dry, 1 cm sections of silicone or latex catheters were suspended between adjacent agar blocks as bridges for inocula on large sections only. No bridges were provided with inocula on smaller blocks, which served as negative controls. The plates were incubated at 37 °C overnight and examined for swarming across the catheter bridges. Eight independent replicates were analyzed (15 catheter sections for each material) and compared using Chi-square Test (Scavone et al., 2016).

2.7. Biofilm formation under different iron availability conditions

The biofilm determination was carried out by a crystal violet staining method adapted from O'Toole & Kolter as described before (O'Toole and Kolter, 1998; Gonzalez et al., 2019; Da Cunda et al., 2020). In order to evaluate the biofilm formation under different iron availability conditions; for iron deprivation LB was supplemented with the metal chelator 22 dipyridyl (200 μM) (Tomaras et al., 2003), while FeCl_3 (15 μM) was used for iron supplementation. The OD values of the negative controls (ODc) were subtracted from the values of the test wells. The score proposed by Villegas et al. (2013) was used to assess the strains ability to form biofilms and it was defined by: $OD \leq ODc$ = no biofilm producer; $ODc < OD \leq (2 \times ODc)$ = weak biofilm producer; $(2 \times ODc) < OD \leq (4 \times ODc)$ = moderate biofilm producer; and $(4 \times ODc) < OD$ = strong biofilm producer. The assay was performed two times and the results were compared using Student Test.

2.8. Expression of genes related with iron acquisition during biofilm development (RT- qPCR)

2.8.1. RNA extraction and quantitative real-time PCR

The wild type Pr2921 was grown in 5 ml of LB broth in six-well flat-bottom plates (Greiner CELLSTAR®) under different iron conditions during 48 h at 37 °C to allow biofilm formation. The different conditions assayed were BF: biofilm formation in LB, DYP: biofilm formation in LB

under iron restriction conditions, with 2'2 dipyridyl at 200 μM , DYP- FeCl_3 : biofilm formation in LB with 2'2 dipyridyl at 200 μM and iron (FeCl_3 15 μM). Planktonic cells were removed by gently washing with PBS. Then, 1 ml of RNA later® (Ambion) was added to the biofilm and RNA extraction was performed using the PureLink® RNA mini kit (Ambion) according to manufacturer recommendations. The total RNA was treated with DNase I (Invitrogen) to remove contaminating genomic DNA. After that, first-strand cDNA was synthesized using random primers and M-MLV Reverse Transcriptase (Invitrogen) according to the manufacturer's recommendation. Specific primers were designed to amplify ferritin and TonB-dependent receptor genes using Primer Blast (Table 1) and *rpoA* RNA polymerase A as housekeeping gene control (Scavone et al., 2016). Syber Green (Invitrogen) fluorescence was used to analyze the results of the quantitative real-time PCR using Biorad Detection System. The amplification program consisted of one cycle of 2 min at 50 °C, 15 min at 95 °C and 40 cycles of 15 s to 94 °C, 30 s at 60 °C and 30 s at 72 °C. Data were normalized to *rpoA* (and analyzed by the threshold cycle ($2^{-\Delta\Delta CT}$) method as described by Livak and Schmittgen (2001). Experiments were performed in triplicate.

2.9. Biofilms characterization by CLSM

The *in vitro* biofilms assays were performed as previously described (Schlapp et al., 2011). The biofilms were grown on coverslips immersed in LB and samples were taken at different time points (1, 3, 5 and 7 days). Then, the coverslips were removed, planktonic cells washed with PBS (x3) and finally the biofilms were fixed with PFA (4%). The immunofluorescence was carried out as described by Schlapp et al., 2011 using the polyclonal anti-Pr2921 serum (primary antibody) and an anti-mouse antibody (secondary antibody) conjugated to fluorescein isothiocyanate (FITC). For nucleic acid staining, DAPI was used.

For imaging such complex microbial communities, we used a confocal laser scanning Olympus BX- 61 FV300 CLS microscope, Fluoview software 4.3, a 100 \times oil immersion objective (NA=1.35), and 488/520 nm and 405/470 nm excitation/emission wavelength for FITC and DAPI respectively. In this microscope, the acquisition step size was of 0.3 μm in the z-axis and 1024 \times 1024 pixels in the xy-plane with a pixel size of 70 nm. The image processing for morpho-topological descriptors was previously described (Schlapp et al., 2011) and the compactness of biofilm was evaluated by the following selected parameters: the number of bacteria per stack, the total bacterial volume, the extracellular material volume and the hexagonal lattice formation (Härtel et al., 2005; Schlapp et al., 2011). For each condition (bacteria strain and day) three representative stacks were taken for quantification of the difference parameters.

2.10. Animal models

Eight-week-old female CD-1 mice were used for all the experiments. All animal procedures were approved by the Bioethics Committee of IIBCE (CEUA), Montevideo, Uruguay, and all experiments were conducted in accordance with CEUA regulations on the use of animals in scientific research.

2.10.1. Experimental ascending urinary tract infection in mice

Mice were anesthetized with xylazine (10 mg/kg) and ketamine (50 mg/kg) before infection. Three groups of 8 mice were transurethrally infected with 2×10^8 cfu of either the *P. mirabilis* 2921-WT strain, or with 2921-50 and 2921-110 mutant strains, in 50 μl of PBS (Zunino et al., 1994). Seven days after the challenge, mice were euthanized and bladders and kidneys were aseptically removed and homogenized separately in 10 ml of PBS with a Stomacher 80 Lab Blender (Seward). Homogenized tissues were plated on Nutrient Agar for the recovery and enumeration of bacteria, and colony counts used to calculate cfu per organ (Zunino et al., 2000).

2.10.2. Experimental catheter associated urinary tract infection (CAUTI) in mice

Mice were anesthetized with xylazine (10 mg/kg) and ketamine (50 mg/kg) before the procedure. Eight groups of 4 mice were used to compare the CAUTI model vs UTI. We performed bacteria counts in urine, bladder weight and histopathology in both models. First, the mice were subjected to soft abdominal massage to induce micturition. Then, in the CAUTI model, a soft 3 mm long polyethylene catheter with an outer diameter of 0.61 mm, was transurethraly introduced and pushed into the bladder with another longer catheter. Through this one, the bacterial suspension was introduced into the bladder as it was previously described (2×10^8 cfu in 50 μ l of PBS). The larger catheter was removed and the small one kept in place (Conover et al., 2015). The UTI model was performed as described before with the difference that animals were sacrificed on day 3 and the bladders were subjected to the same analyses as in CAUTI model. Urine cultures were performed just before the mice were sacrificed. Three days after the challenge, mice were euthanized and the bladders were removed for histological sectioning and the weight of the bladder were also measured for both models.

Then, bladders were embedded in Tissue Freezing Medium (Leica Biosystems). After that, all samples were sectioned, stained with hematoxylin and eosin and examined microscopically (Umpierrez et al., 2013). Bladder sections (12 μ m) were analyzed using a light microscope OLYMPUS DP71 and CellF program (OLYMPUS). The intensity of the damage was quantified using the semiquantitative score described by Alamuri et al. (2009) and previously used by our group (Umpierrez et al., 2013) and compared using Tukey's multiple comparison test.

2.11. Statistical analyses of data

All data were analyzed using Prism version 6.0c for Mac OS X (GraphPad Software Inc., USA). Student's t-test or the non-parametric equivalent Mann-Whitney test were used to assess animal experiments results. Data regarding migration over catheter bridge sections was analyzed using the Chi-Square test.

3. Results

3.1. Isolation and characterization of biofilm-deficient mutants

From a collection of 5952 transconjugants (derived from the wild type clinical isolate *P. mirabilis* 2921), only 53 mutants exhibited differences in biofilm formation (either deficiency or enhancement compared to the WT), although growth was not affected. After Southern blot analyses only 12 mutants from the 53 have a unique Tn insertion. Genes disrupted in 12 of these mutants (9 biofilm formation deficient (BFD), and 3 biofilm formation enhanced (BFE) Fig. 1A) were identified by sequencing of the chromosomal DNA flanking Tn inserts, and comparison with the *P. mirabilis* HI4320 genome (Pearson et al., 2008, Supplementary Table S1).

Two out of the 12 mutated genes were related with iron metabolism. The mutant 2921-50 showed the non-heme ferritin gene, PMI_RS04890 disrupted, and 2921-110 the TonB-dependent receptor gene, PMI_RS18440 disrupted (Table 2, Supplementary Table S1). To confirm that the disrupted genes accounted for the phenotype of the mutants, the expression of the downstream genes was first assessed to rule out any potential polar effects associated with the mini-Tn insertion. Quantitative real-time (qRT)-PCR showed that expression of genes immediately downstream from the disrupted PMI_RS04890 locus in 2921-50 and PMI_RS18440 in 2921-110 was not affected, confirming that the biofilm phenotypes were due to the disruption of each gene (Supplementary Figs. S1 and S2).

3.2. Motility and hydrophobicity characterization

No significant differences in swimming motility were observed

among the mutant strains compared with the wild type having all of them a value of $2.6 \text{ cm} \pm 0.29 \text{ cm}$ (Fig. 1B). However, in the case of swarming, a significant decrease was observed between the 2921-110 mutant strain and the 2921-WT (12.5 cm^2 , 50 cm^2 , $P \leq 0.01$, Fig. 1C). When hydrophobicity was assayed, we observed a significant increase in the hydrophobicity index of the 2921-50 cells (22.46) over the strain 2921-WT (18.49 $P \leq 0.05$, Fig. 1D). When the capability of wild type (2921), and mutant strains 2921-50 and 2921-110 to migrate over different catheter materials were assayed, a significant decrease in the migration was observed for the 2921-110 mutant strain in both latex and silicone materials (53.3%, 40%, respectively) in comparison with the 2921-WT (86.7% 93.3% $P \leq 0.01$, $P \leq 0.001$, respectively, Fig. 1E).

3.3. Iron could trigger biofilm increase

The effects of different iron conditions on biofilms formation were assessed using the semi quantitative technique based on the adsorption of associated crystal violet. First we assessed the effect of iron restriction on biofilm formation in the 2921-WT strain by addition of increasing concentrations of the iron chelator 2,2-dipyridyl from 100 to 500 μ M. The result showed that 200 μ M had an effect on planktonic cells growth but it was improved by the addition of FeCl₃ (Supplementary Fig. S3). With 300–500 μ M the growth was inhibited and with 100 μ M we did not observe differences with the cell without iron restriction (Supplementary Fig. S3).

In our work, the wild type 2921-WT showed similar biofilms biomasses ($0.9\text{--}1.22 \pm 0.26$) in the different conditions, while the highest amount was observed in iron supplementation condition (1.48 ± 0.12) but not significant differences were obtained (Fig. 2). The mutant in ferritin gene (2921-50) showed a significant biomass increase in the presence of iron supplementation (2.05 ± 0.21 , $P \leq 0.001$). In the case of the TonB-dependent receptor mutant (2921-110) in both conditions, we observed a significant increase in biomass production in restriction of iron (0.89 ± 0.19) and also a significant biomass production in iron-supplemented condition (0.99 ± 0.18 , $P \leq 0.05$, $P \leq 0.01$, respectively) compared with LB (0.28 ± 0.06). It is interesting to note that while planktonic cells were affected by the concentration of 2,2-dipyridyl, the biofilm biomass increased in this condition. The results suggest that biomass biofilm formation in *P. mirabilis* 2921 is iron responsive and that the ferritin and TonB-dependent receptor genes are involved in this response.

3.4. Expression of iron genes is variable during iron starvation

In order to determine the role of the ferritin- and TonB-dependent receptor genes during biofilm formation, their expression levels were quantified by qRT-PCR under different iron availability conditions. In the biofilm, the expression of the TonB-dependent receptor gene was significantly increased under iron restriction conditions (relative fold change 7.94) compared with the expression in bacteria grown in unmodified LB (relative fold change 1, $P \leq 0.05$, Fig. 3). When iron was added, the expression of this gene decreased (relative fold change 4.08) compared with the restriction condition, but the expression was significantly higher than that observed in normal media (LB) ($P \leq 0.05$, Fig. 3). In the case of the ferritin expression we did not observe significant variations in the conditions assayed.

3.5. Complexity of the biofilm

The evolution of the biofilm along time was analyzed using the three strains. The morpho-topological parameters revealed clear differences among the mutants and the wild type strain (Fig. 4. A–C). While the 2921-110 mutant strain did not produce a biofilm at any stage in LB, the 2921-50 produced a big biofilm at day 1 and 3 while at day 5 the biofilm diminished. We were not able to observe extracellular matrix in these two mutant strains during the entire time process (Fig. 4C).

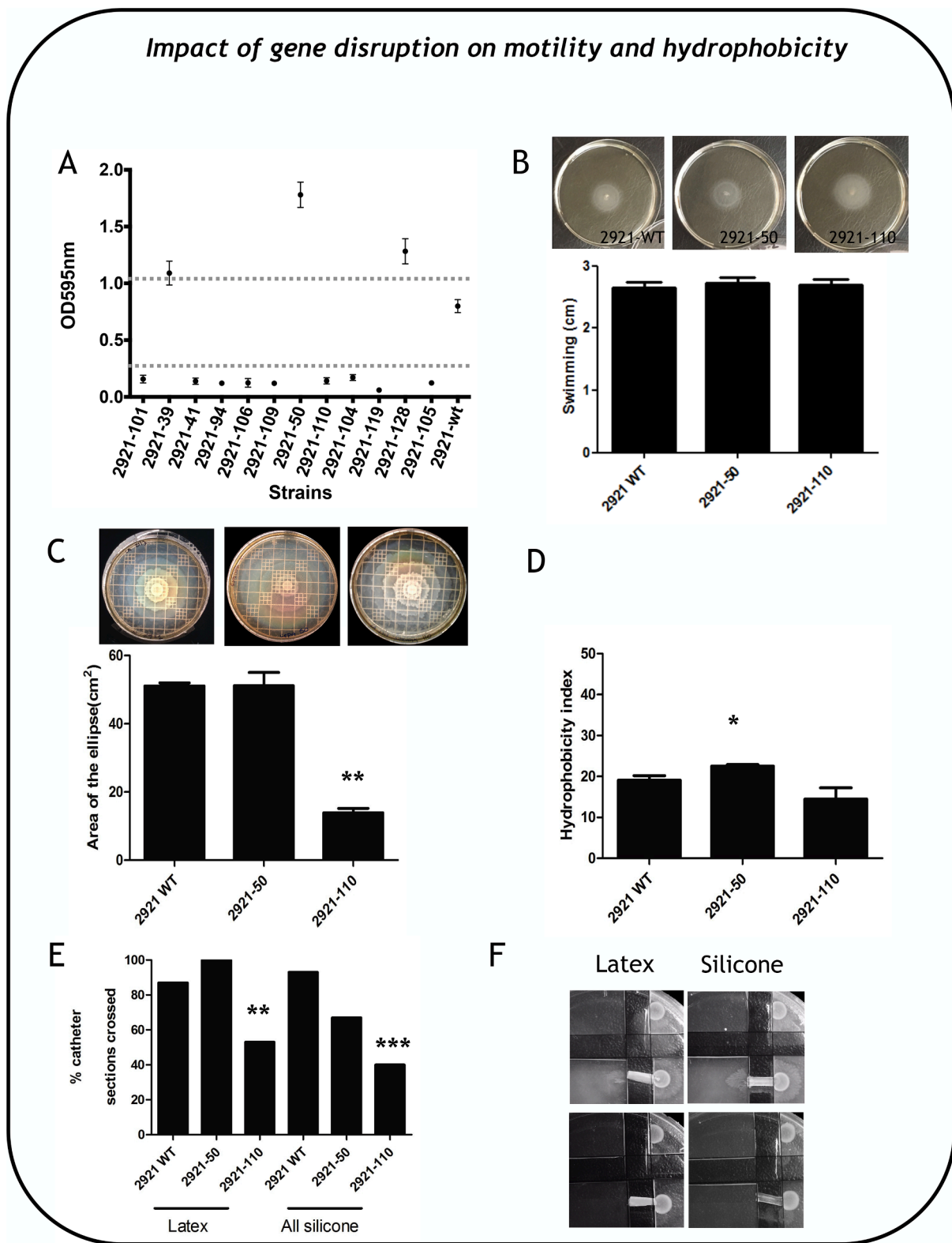


Fig. 1. Impact of gene disruption on motility and hydrophobicity. (A) Biofilm screening in the selected mutant strains. (B) Comparison of ability or wild type *P. mirabilis* 2921 and mutants in swimming motility. (C) Comparison of ability or wild type *P. mirabilis* 2921 and mutants in swarming motility, Student test ** $P \leq 0.01$ 2921-WT vs mutant strain. (D) Cell surface hydrophobicity of *P. mirabilis* 2921 and mutants were measured using Hydrocarbon (xylene) * $P = 0.0152$ Kruskal-Wallis Test. (E) Comparison of ability or wild type *P. mirabilis* 2921 and mutants to migrate over sections of latex or silicone catheters. Data show percentage of catheter sections crossed from 15 replicates. Error bars shown SEM. * $P \leq 0.05$, ** $P \leq 0.01$, *** $P \leq 0.001$ 2921-WT vs mutant strain. (F) Representative images of migration/no migration over latex (left) and silicone (right).

Table 2.

Bacterial strains and their main characteristics.

Strain	Description	Biofilm formation	Sources/ Reference
Pr2921	Clinical isolate, patient with symptomatic UTI	High	Zunino et al. (2000)
50	2921-50 mutant in PMI_RS04890	Enhanced	This work
110	2921-110 mutant in PMI_RS18440	Deficient	This work

The hexagonal lattice model is a good predictor of compactness and complexity of the biofilm (Schlapp et al., 2011). The analysis of the models for each strain showed that the wild type followed an increase in complexity until day 5 followed by a dispersion step (Fig. 5). In the case of ferritin mutant strain (2921-50), the biofilm complexity had its maximum on day 3 suggesting an early dispersion. On the other hand, the TonB-dependent receptor mutant (2921-110) never reached a similar level of complexity during all 7 days. These two mutants did not follow the steps of the wild type strain as we know under the conditions evaluated here (Fig. 5).

3.6. Impaired iron acquisition reduced the urinary tract colonization

In order to analyze the contribution of both mutants in the colonization of the urinary tract, two experimental mice models were used. When the classical ascending UTI model was used, both mutant strains (2921-50 and 2921-110) were recovered in significantly lower levels from kidneys and bladders compared with the wild type strain (2921-WT) ($P \leq 0.05$ in all cases, Fig. 6A).

In the case of the catheter urinary tract infection (CAUTI) model, two parameters of infection were evaluated: log cfu/ml in urine and bladder weight (Fig. 6B, C). In the CAUTI model it was not possible to assess the values of CFU in the organs as the tissues were cryopreserved in order to evaluate the histological damage. Three days after infection, almost all groups of mice had similar values of CFU in urine. The 2921-WT showed the highest values of cfu/ml in urine, while 2921-50 had a decrease in the values the differences were not significant. In the case of 2921-110 we have observed a significant diminish from 1.7 Log₁₀ cfu/ml in urine compared with the values of 5 Log₁₀ cfu/ml in 2921-WT ($P \leq 0.01$). This result suggests that the ability of 2921-110 to colonize a catheterized urinary tract is impaired.

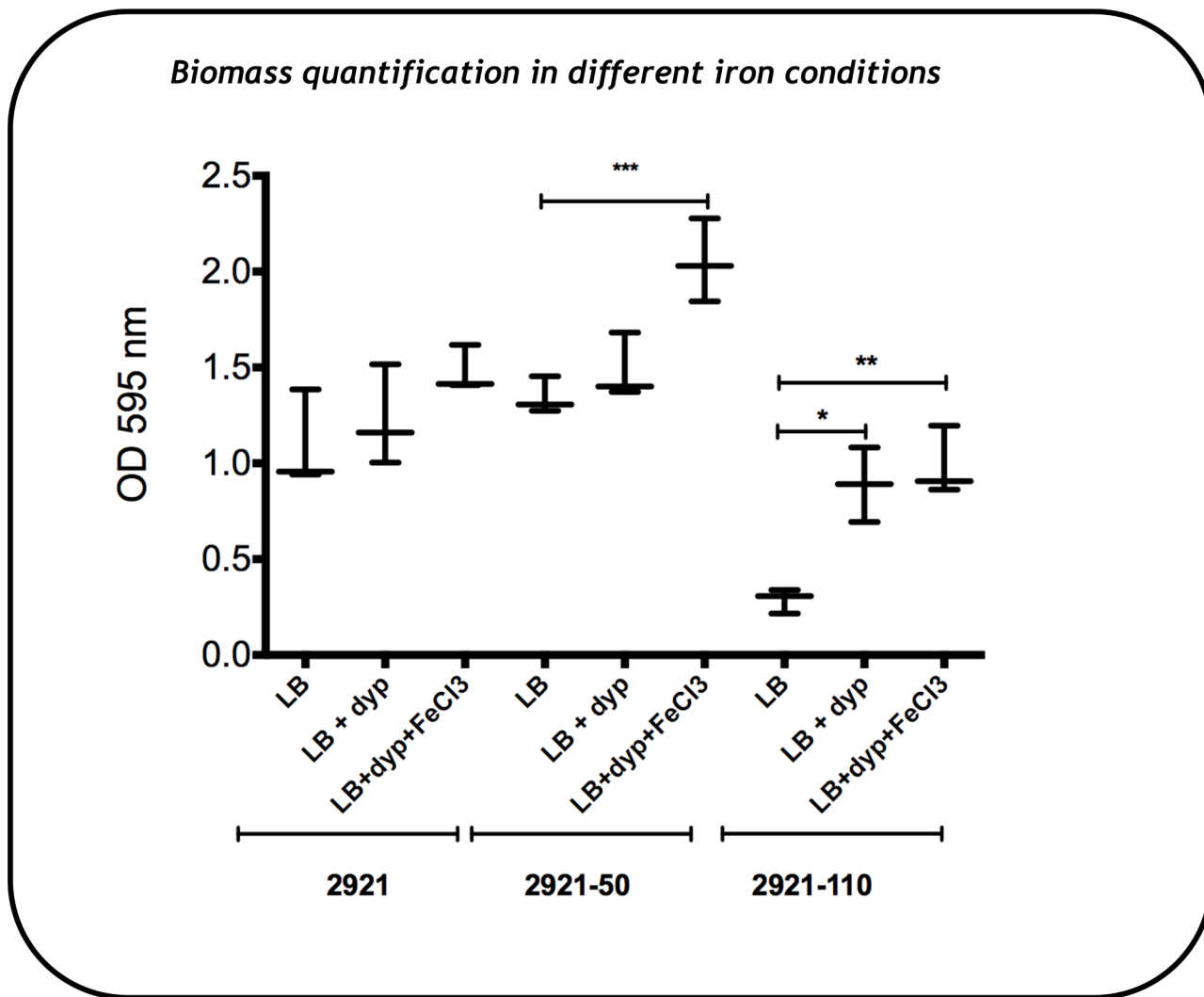


Fig. 2. Biomass quantification in different iron conditions. *P. mirabilis* 2921 WT strain showed similar biofilms biomass in the different conditions. 2921-50 (mutant in ferritin gene) showed a significant increase in biomass in the presence of iron (dyp- FeCl₃). 2921-110 (mutant in Ton B associated porin protein mutant) had and increase in biomass production in restriction of iron and also a highest biomass production in iron supplementation condition. Error bars shown SEM. * $P \leq 0.05$, ** $P \leq 0.01$, *** $P \leq 0.001$ 2921-WT vs mutant strain (Student test).

dyp: 2'2 dipyrindyl (iron chelating agent) at 200 μ M

Iron source: FeCl₃ 15 μ M.

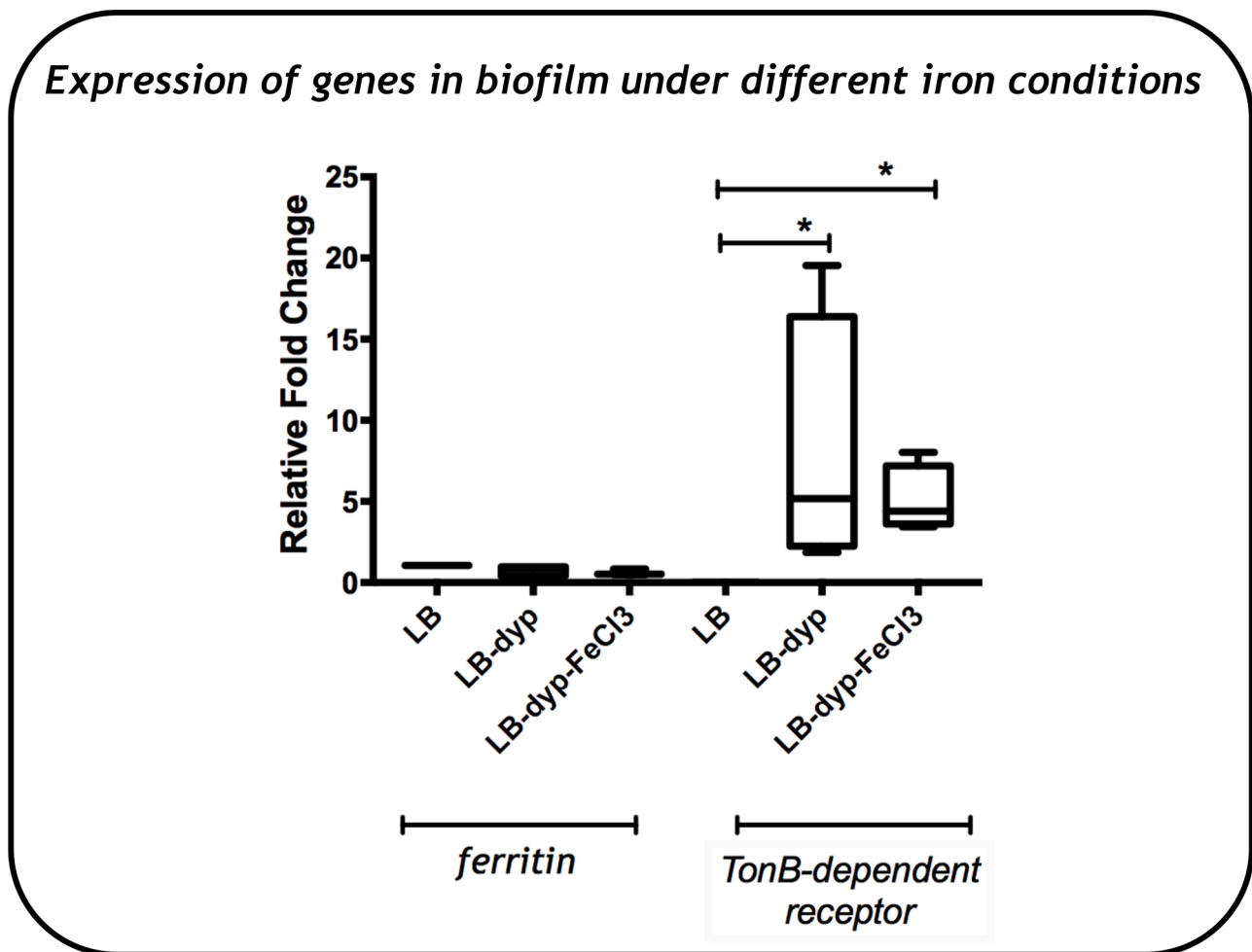


Fig. 3. Expression of genes in biofilm under different iron conditions.

Relative fold difference in the expression of ferritin and TonB associated porin protein obtained by quantitative real-time PCR. The TonB-associated porin protein gene was significantly increased under iron restriction conditions compared with the expression in bacteria grown in LB (* $P \leq 0.05$ Student test). When iron was added, the expression of this gene decreased compared with the restriction condition. In the ferritin expression we do not observe significant variations in the conditions assayed.

LB: biofilm formation in LB broth

DYP: biofilm formation in LB under iron restriction condition with 2'2 dipyrldyl (200 μ M)

DYP-FeCl₃: biofilm formation in LB under iron restriction (200 μ M DYP) and supplemented with iron (FeCl₃ 15 μ M).

The size of the bladder is a parameter that reflects the degree of infection (Ambruster et al., 2018). The results confirmed that the infection of the bladder with the presence of the catheter produced the biggest bladder sizes (0.07 g, Fig. 6C). In the case of the mutant strains, the 2921-110 did not induce an increase in the bladder size neither in UTI nor in CAUTI model (≤ 0.03 g). The size of the bladder of mice infected with 2921-110 was also similar to the naive bladder (0.04 g) without infection (Fig. 6C), suggesting that the mutant strain is impaired in infection. In order to confirm the observation of the bladder weight, histological sectioning and staining was performed in the murine bladders after UTI and CAUTI model. The damage was quantified using the bladder histological modification score as previously described (Umpierrez et al., 2013). In the CAUTI model we observed significant differences in the score of damage caused by 2921-110 (0–0.5) compared with the 2921 wild-type (2.5–3) and also with the 2921-50 (1.5–2.5, $P = 0.0001$ in both cases, Fig. 6D). When the score of damage in CAUTI 2921-110 was compared with the one observed in mice only catheterized (0.5), we did not observe any significant differences. In the case of 2921-50 CAUTI model, the damage was not significantly different to the one observed in 2921 challenged mice and it was significantly higher than the control (catheterized mice). In Fig. 7, the

histopathological sectioning of murine bladder stained with hematoxylin and eosin is shown. In panel A, a normal bladder morphology (naive) is shown, where the bladder lumen, the transitional epithelium, the lamina propria, and the muscle tissue can be clearly identified. In the case of the bladder with 2921-WT UTI (panel B) the bladder was bigger, thickened transitional epithelium and infiltrated cells could be observed. In UTI with 2921-50 (panel C) the damage of the bladder was not different to that exerted by the wild-type 2921. In the case of 2921-110 (panel D), we were not able to observe any tissue damage and the bladder size was similar to naive mice (panel A).

In the CAUTI model we observed an increased damage in bladder tissues, probably due to the presence of the catheter into the bladder that causes major histopathological changes in the bladder (Fig. 7 panel A). Bladder histology of catheterized mice without bacteria showed more damage compared with naive bladder (Fig. 7 panel A) confirming that the presence of the catheter alone was causing some damage. CAUTI 2921-WT (Panel B) and CAUTI 2921-50 (Panel C) presented bigger bladders (Fig. 6 panel C) with histological damage, thickened transitional epithelium and infiltrated cells. CAUTI 2921-110 (Panel D) did not show any signal of damage produced by bacteria and it was similar to the naive control bladder (naive Panel A) so we could infer that the

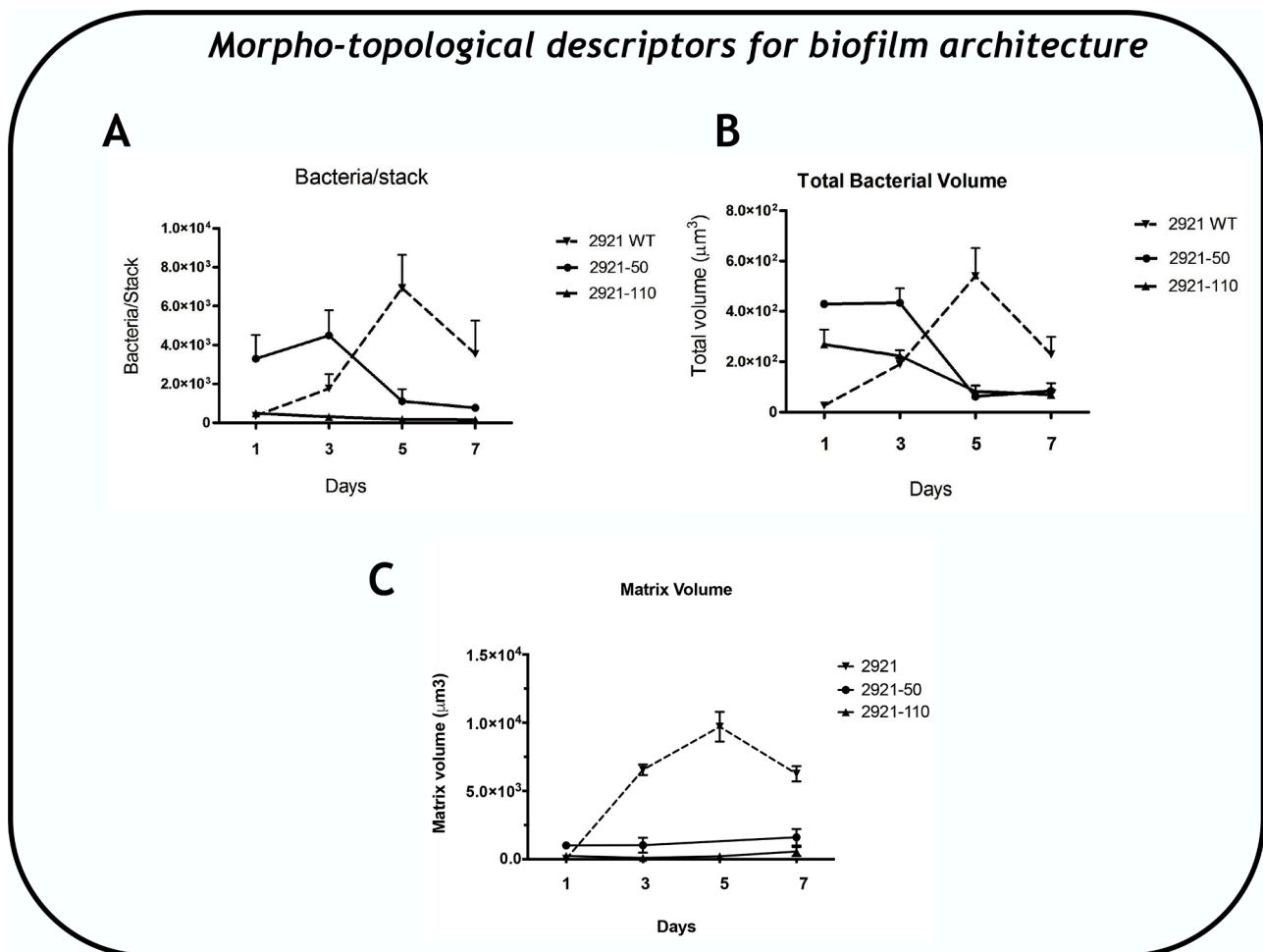


Fig. 4. Morpho-topological descriptors for biofilm architecture. (A) Number of bacteria per stack. (B) Total bacterial volume per stack. (C) Matrix volume per stack. Symbols represent mean values of 3 independent experiments. Error bars represents standard errors. 2921:wild type strain, 2921-50: 2921-ferritin-mutant strain, 2921-110—TonB associated porin protein mutant.

damage was only produced by catheterization in the case of this strain.

4. Discussion

It is estimated that about 65% of all bacterial infections are associated with bacterial biofilms (Lewis, 2001). Bacterial pathogens sense iron-limiting conditions and respond accordingly by up-regulating iron-acquisition mechanisms and virulence genes (Zughaier and Cornelis, 2018). The urinary tract is an iron-restricted environment (Shand et al., 1985), *P. mirabilis* can grow under iron restriction because encodes iron scavenging and uptake systems that are induced during infection (Pearson et al., 2008; Himpfl et al., 2010; Pearson et al., 2011). Few studies have revealed the role of iron system acquisition in biofilms formation. Because of the potential importance of biofilms of *P. mirabilis* during infection (Schaffer and Pearson, 2017), we have examined how two iron systems affect the biofilms formation in different models.

One of the mutants used in this study (2921-50) had interrupted the gene that encodes for non heme ferritin. Ferritin of different organisms are involved in a range of functions including iron regulation, mono-oxygenation, and reactive radical production. In the experiments carried out in this study, we observed that the motility of 2921-50 strain was not affected, compared with the wild type strain. In addition, we observed that biofilm development occurred in early stages (day 1 and day 3) when the highest degree of compaction was seen. We observed that the mutant strain (2921-50) was able to establish and develop a biofilm in the first few days, but it was rapidly destabilized. Ferritin

could probably have a relevant role in later stages of biofilm development and therefore does not follow the pattern observed in the wild strain. In this context, we hypothesize that ferritin, as an iron storage protein, could be relevant for the late stages of the biofilm. As the available iron in the medium is consumed, the bacteria need the reservoir and as it was demonstrated in this work, the absence of ferritin caused a rapid dispersion of the biofilm. 2921-50 was unable to colonize the urinary tract in the UTI model. In the case of the CAUTI model, 2921-50 damaged the bladder similarly to wild type. It is possible that the damage induced by the catheter helps the bacteria to gain access to the bladder tissues and to iron. Moreover, the catheter itself could serve as abiotic surface for the biofilms formation and this would explain the results observed in the CAUTI model.

The 2921-110 strain, was mutated in one of the tonB-dependent receptor (PMI_RS18440). This strain showed an impaired swarming motility compared to the wild-type, and was not able to develop a stable biofilm over time in our static biofilm formation model. We propose that in this case, the mutation causes the absence of a TonB-associated receptor protein that would affect the bacterial membrane and therefore impairs its mobility capacity. *P. mirabilis* encodes at least 21 putative iron acquisition systems and 15 genes related to TonB-dependent receptors (Pearson et al., 2008; Himpfl et al., 2010). The strain could not probably adhere properly in the initial stages of biofilm development and therefore did not achieve a stable biofilm. In addition, 2921-110 failed to colonize the urinary tract in UTI and CAUTI models. Studies on uropathogenic *E. coli* have shown that the urinary tract is iron-limited

Complexity of the biofilm represented by hexagonal lattice model

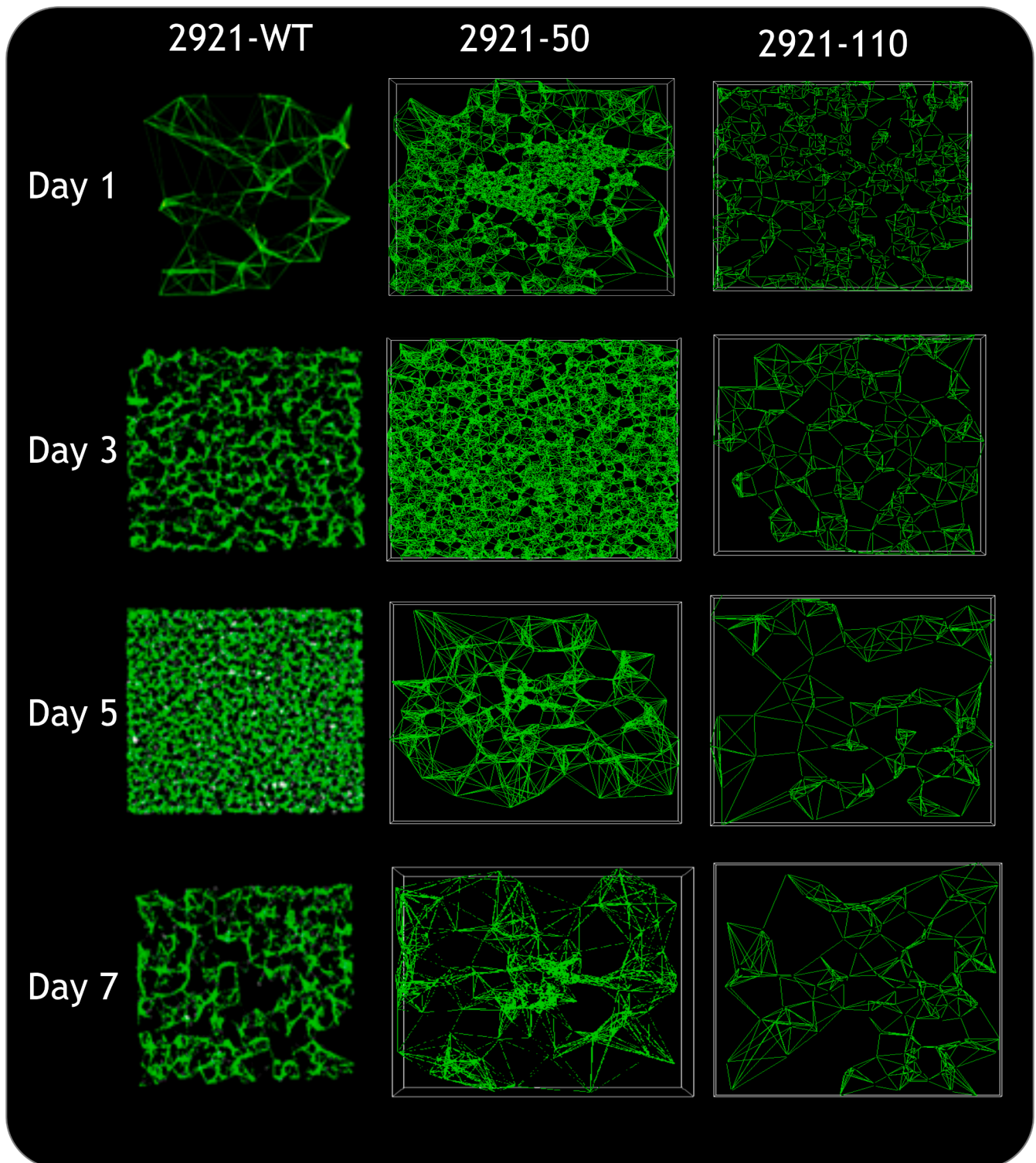


Fig. 5.. Complexity of the biofilm represented by hexagonal lattice model. 2921:wild type strain, 2921-50 —ferritin-mutant strain, 2921-110- TonB associated porin protein mutant. Each line represent the distance between one bacteria and its six more close neighbors.

and that iron acquisition by outer membrane receptors is important during UTI (Torres et al., 2001; Snyder et al., 2004; Alteri and Mobley, 2007; Hagan and Mobley, 2009).

The importance of iron uptake systems in the colonization of the urinary tract has been observed in studies where mutants of *P. mirabilis*

with an interruption in the *nrp* gene. In that study, a co-challenge experiment was carried out and found that the mutant strain did not achieve colonization of the bladder or kidneys (Himpl et al., 2010). *P. mirabilis* encodes iron systems acquisitions that are induced during the UTI, Burall et al. (2004) found five genes to be associated with iron

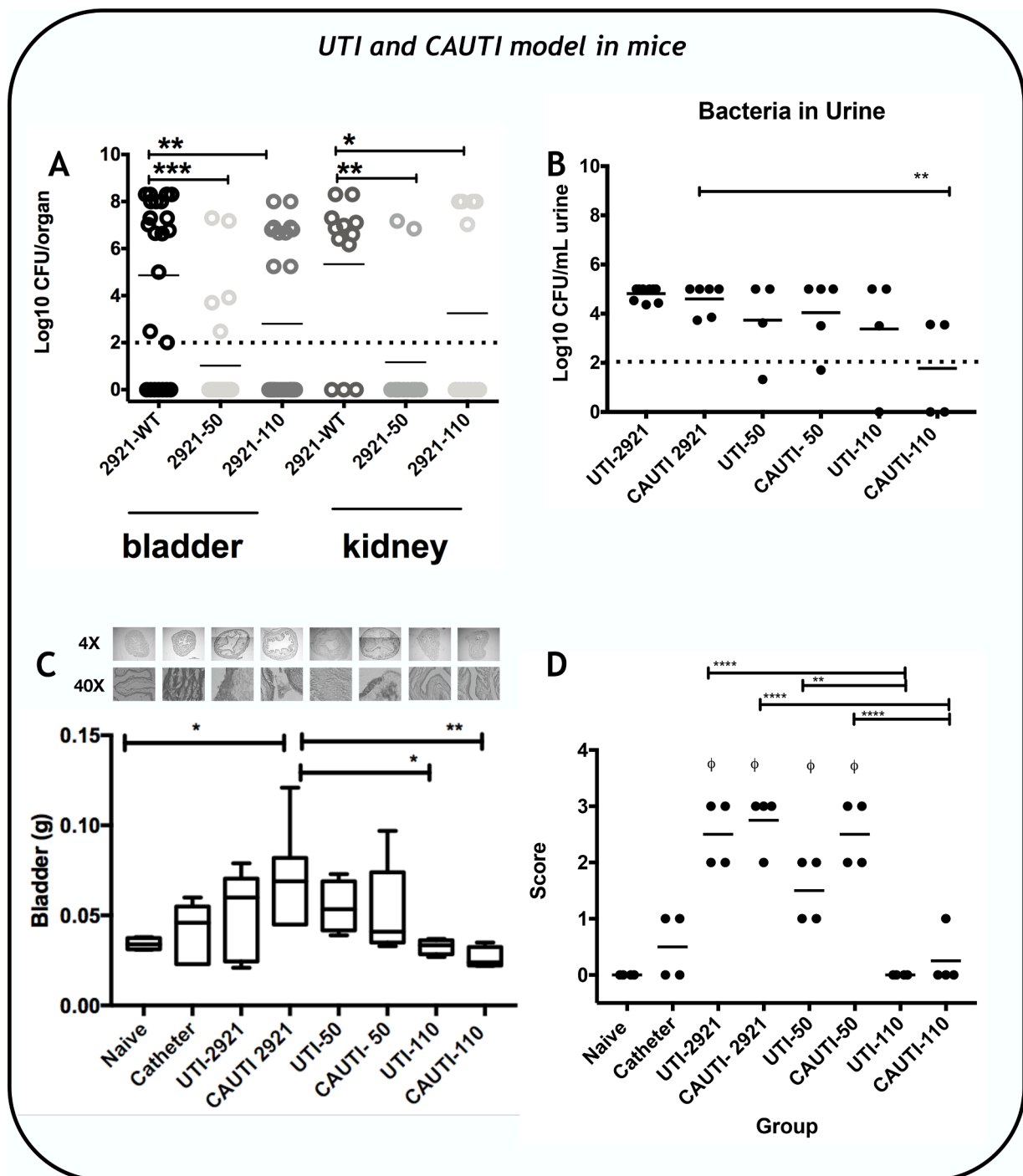


Fig. 6. *UTI and CAUTI model in mice.* (A) Levels of viable bacterial cells recovered from bladders and kidneys after experimental infection, data are presented as Log₁₀ CFU per organ. * $P \leq 0.05$; ** $P \leq 0.01$; **** $P \leq 0.0001$, Mann-Whitney Test 2921-WT Vs 2921-50 and 2921-110. The dot line represents the limit of detection. (B) Number of viable cells present in residual urine in bladders of UTI and CAUTI models, data are presented as Log CFU per ml urine ** $P \leq 0.01$. Mann-Whitney Test. The dot line represents the limit of detection. (C) Comparison of bladder weight of UTI and CAUTI models. Above the graph, representative images of all samples sectioned, stained with hematoxylin and eosin. Bladder sections were analyzed using a light microscope OLYMPUS DP71 and CellF program (OLYMPUS). Error bars represents the standard error of the mean, * $P \leq 0.05$; ** $P \leq 0.01$; **** $P \leq 0.0001$ Student T-test. (D) Score of histopathology damage in the different groups. ** $P \leq 0.01$; **** $P \leq 0.0001$ Tukey's Multiple Comparison Test, ϕ difference between infected group (either UTI or CAUTI) and their, respectively control group (naive and catheter).

acquisition result in attenuation of virulence when they are mutated. Himpls et al. (2010) demonstrated using microarray analysis that *P. mirabilis* cultured under iron limitation has 45 significantly up-regulated genes and 21 represent putative iron-regulated systems. The effect of the iron in biofilms formation had been reported in *E. coli*, where Hancock et al. (2008) observed that the addition of iron during

biofilm formation under iron-limiting conditions significantly increased the amount of biofilm, while the addition of an iron chelator reduced biofilm formation (Hancock et al., 2008).

Under biofilm restriction our results shown an increase in the biofilms formation probably due to the adaptation of this bacteria to an iron limiting condition as it is in the urinary tract (Neidhardt, 1987). Even

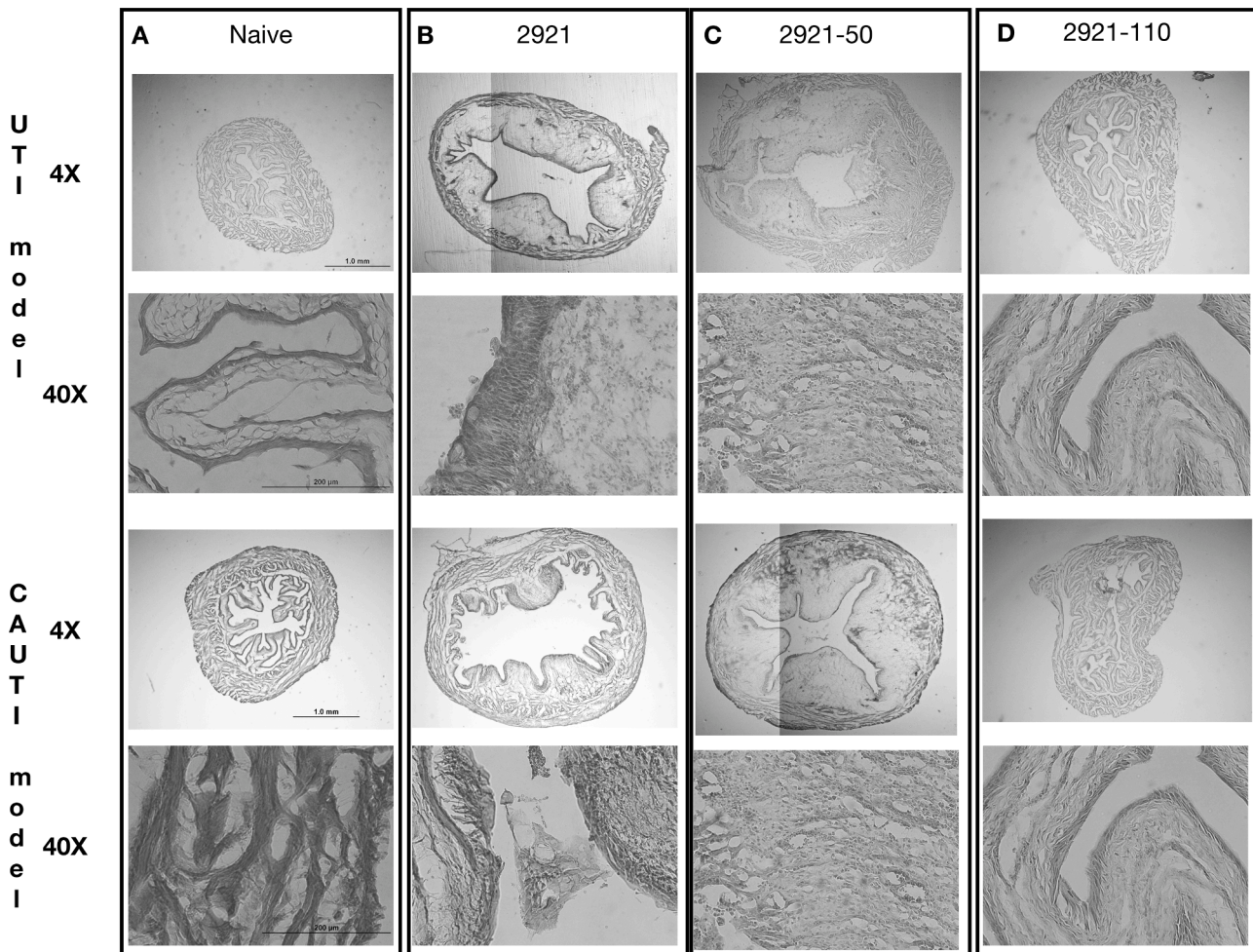


Fig. 7.. Histopathological sectioning of murine bladder stained with hematoxylin and eosin in UTI and CAUTI model. In panel (A) normal bladder morphology (naive), (B) Wild type 2921 UTI (upper image) and CAUTI (bottom image), (C) Mutant strain 2921–50 UTI (upper image) and CAUTI (bottom image), and (D) Mutant strain 2921–110 UTI (upper image) and CAUTI (bottom image).

more, our results shown that the strain was neither able to produce *in vitro* biofilm nor infect the urinary tract. On the other hand, if the biofilm is produced, this would lead to an advantage when an abiotic surface is available as in the CAUTI model.

4.1. Conclusion

Different iron acquisition systems in *P. mirabilis* are relevant for biofilm formation and infection (Jacobsen et al., 2008). The results obtained in the present work confirm the relevant role of ferritin and a TonB-associated porin protein in these two processes. Biofilm formation is a relevant virulence factor in the development of catheter associated urinary tract infection. Inhibition of bacterial iron acquisition could be evaluated by catheter coating with chelators in order to prevent biofilm formation and further infection, but more work is needed to elucidate this issue.

CRediT authorship contribution statement

V Iribarnegaray: Conceptualization, Methodology, Data curation, Writing – original draft. **MJ González:** Methodology, Data curation. **AL Caetano:** Methodology, Data curation. **R Platero:** Methodology, Supervision, Conceptualization, Writing – review & editing. **P Zunino:** Supervision, Conceptualization, Writing – review & editing. **P Scavone:** Supervision, Conceptualization, Methodology, Data curation, Writing – review & editing.

Declaration of Competing Interest

The authors declare that they have no known competing financial interests or personal relationships that could have appeared to influence the work reported in this paper.

Acknowledgements

The authors declare no conflicts of interest.

Funding

This work was funded by Grant FCE-104760 awarded by ANII, Uruguay

Supplementary materials

Supplementary material associated with this article can be found, in the online version, at [doi:10.1016/j.crmicr.2021.100060](https://doi.org/10.1016/j.crmicr.2021.100060).

References

- Alamuri, P., Eaton, K.A., Himpel, S.D., Smith, S.N., Mobley, H.L., 2009. Vaccination with proteus toxic agglutinin, a hemolysin-independent cytotoxin *in vivo*, protects against *Proteus mirabilis* urinary tract infection. *Infect. Immun.* 77 (2), 632–641.

- Alteri, C.J., Mobley, H.L., 2007. Quantitative profile of the uropathogenic *Escherichia coli* outer membrane proteome during growth in human urine. *Infect. Immun.* 75 (6), 2679–2688.
- Armbruster, C.E., Mobley, H.L., Pearson, M.M., 2018. Pathogenesis of *Proteus mirabilis* infection. *Ecosal Plus* 8 (1).
- Bibiloni, R., Pérez, P.F., Garrote, G.L., Disalvo, E.A., De Antoni, G.L., 2001. Surface characterization and adhesive properties of bifidobacteria. *Methods Enzymol.* 336, 411–427.
- Bullen, J.J., Rogers, H.J., Griffiths, E., 1978. Role of iron in bacterial infection. *Curr. Top. Microbiol. Immunol.* 1–35.
- Bullen, J.J., Griffiths, E., Edmiston, C.E., 1999. Iron and infection: molecular, physiological and clinical aspects. 2nd Edition 12 (5), 410.
- Burall, L.S., Harro, J.M., Li, X., Lockett, C.V., Himpf, S.D., Hebel, J.R., Mobley, H.L., 2004. *Proteus mirabilis* genes that contribute to pathogenesis of urinary tract infection: identification of 25 signature-tagged mutants attenuated at least 100-fold. *Infect Immun* 72 (5), 2922–2938.
- Conover, M.S., Flores-Mireles, A.L., Hibbing, M.E., Dodson, K., Hultgren, S.J., 2015. Establishment and characterization of UTI and CAUTI in a mouse model. *J. Vis. Exp. Jove* (100), e52892. <https://doi.org/10.3791/52892>.
- Crichton, R., 2016. Iron Metabolism: From Molecular Mechanisms to Clinical Consequences. John Wiley & Sons.
- Da Cunda, P., Iribarnegaray, V., Papa-Ezdra, R., Bado, I., González, M.J., Zunino, P., Scavone, P., 2020. Characterization of the different stages of biofilm formation and antibiotic susceptibility in a clinical *Acinetobacter baumannii* strain. *Microb. Drug Resist.* 26 (6), 569–575.
- Flores-Mireles, A.L., Walker, J.N., Caparon, M., Hultgren, S.J., 2015. Urinary tract infections: epidemiology, mechanisms of infection and treatment options. *Nat. Rev. Microbiol.* 13 (5), 269–284.
- Giorello, F.M., Romero, V., Farias, J., Scavone, P., Umpiérrez, A., Zunino, P., Silveira, J. S., 2016. Draft genome sequence and gene annotation of the uropathogenic bacterium *Proteus mirabilis* Pr2921. *Genome Announc.* 4 (3), e00564. -16.
- González, M.J., Da Cunda, P., Notejane, M., Zunino, P., Scavone, P., Robino, L., 2019. Fosfomycin tromethamine activity on biofilm and intracellular bacterial communities produced by uropathogenic *Escherichia coli* isolated from patients with urinary tract infection. *Pathog. Dis.* 77 (3), ftz022.
- Hagan, E.C., Mobley, H.L., 2009. Haem acquisition is facilitated by a novel receptor Hma and required by uropathogenic *Escherichia coli* for kidney infection. *Mol. Microbiol.* 71 (1), 79–91.
- Hancock, V., Ferrieres, L., Klemm, P., 2008. The ferric yersiniabactin uptake receptor FyuA is required for efficient biofilm formation by urinary tract infectious *Escherichia coli* in human urine. *Microbiol* 154 (1), 167–175.
- Hantke, K., 2001. Iron and metal regulation in bacteria. *Curr. Opin. Microbiol.* 4 (2), 172–177.
- Härtel, S., Fanani, M.L., Maggio, B., 2005. Shape transitions and lattice structuring of ceramide-enriched domains generated by sphingomyelinase in lipid monolayers. *Biophys. J.* 88 (1), 287–304.
- Himpf, S.D., Pearson, M.M., Arewång, C.J., Nusca, T.D., Sherman, D.H., Mobley, H.L., 2010. Proteobactin and a yersiniabactin-related siderophore mediate iron acquisition in *Proteus mirabilis*. *Mol. Microbiol.* 78 (1), 138–157.
- Holling, N., Lednor, D., Tsang, S., Bissell, A., Campbell, L., Nzakizwanayo, J., Salvage, J. P., 2014. Elucidating the genetic basis of crystalline biofilm formation in *Proteus mirabilis*. *Infect. Immun.* 82 (4), 1616–1626.
- Jacobsen, S.M., Stickler, D.J., Mobley, H.L.T., Shirtliff, M.E., 2008. Complicated catheter-associated urinary tract infections due to *Escherichia coli* and *Proteus mirabilis*. *Clin. Microbiol. Rev.* 21 (1), 26–59.
- Jones, B.V., Young, R., Mahenthalingam, E., Stickler, D.J., 2004. Ultrastructure of *Proteus mirabilis* swarmer cell rafts and role of swarming in catheter-associated urinary tract infection. *Infect. Immun.* 72 (7), 3941–3950.
- Lewis, K., 2001. Riddle of biofilm resistance. *Antimicrob. Agents Chemother.* 45 (4), 999–1007.
- Litwin, C.M., Calderwood, S.B., 1993. Role of iron in regulation of virulence genes. *Clin. Microbiol. Rev.* 6 (2), 137–149.
- Livak, K.J., Schmittgen, T.D., 2001. Analysis of relative gene expression data using real-time quantitative PCR and the 2⁻ΔΔCT method. *Methods* 25 (4), 402–408.
- Maniatis, T., Fritsch, E.F., Sambrook, J., 1982. Molecular cloning: a Laboratory Manual, 545. Cold Spring Harb Protoc, Cold Spring Harbor, NY.
- Martínez-García, E., Calles, B., Arévalo-Rodríguez, M., De Lorenzo, V., 2011. pBAM1: an all-synthetic genetic tool for analysis and construction of complex bacterial phenotypes. *BMC Microbiol.* 11 (1), 38.
- O'Hara, C.M., Brenner, F.W., Miller, J.M., 2000. Classification, identification, and clinical significance of *Proteus*, *Providencia*, and *Morganella*. *Clin. Microbiol. Rev.* 13 (4), 534–546.
- O'Toole, G.A., Kolter, R., 1998. Initiation of biofilm formation in *Pseudomonas fluorescens* WCS365 proceeds via multiple, convergent signalling pathways: a genetic analysis. *Mol. Microbiol.* 28 (3), 449–461.
- Pearson, M.M., Sebaihia, M., Churcher, C., Quail, M.A., Seshasayee, A.S., Luscombe, N. M., Hauser, H., 2008. Complete genome sequence of uropathogenic *Proteus mirabilis*, a master of both adherence and motility. *J. Bacteriol.* 190 (11), 4027–4037.
- Pearson, M.M., Yep, A., Smith, S.N., Mobley, H.L., 2011. Transcriptome of *Proteus mirabilis* in the murine urinary tract: virulence and nitrogen assimilation gene expression. *Infect. Immun.* 79 (7), 2619–2631.
- Pratt, L.A., Kolter, R., 1998. Genetic analysis of *Escherichia coli* biofilm formation: roles of flagella, motility, chemotaxis and type I pili. *Mol. Microbiol.* 30 (2), 285–293.
- Scavone, P., Iribarnegaray, V., Caetano, A.L., Schlapp, G., Härtel, S., Zunino, P., 2016. Fimbriae have distinguishable roles in *Proteus mirabilis* biofilm formation. *Pathog Dis* 74 (5).
- Schaffer, J.N., Pearson, M.M., 2017. *Proteus mirabilis* and urinary tract infections. *Urin. Tract Infect. Mol. Patho. Clin. Manag.* 3 (5), 383–433.
- Schlapp, G., Scavone, P., Zunino, P., Härtel, S., 2011. Development of 3D architecture of uropathogenic *Proteus mirabilis* batch culture biofilms—A quantitative confocal microscopy approach. *J. Microbiol. Methods* 87 (2), 234–240.
- Shand, G.H., Anwar, H., Kadurugamuwa, J.A.G.A.T.H., Brown, M.R., Silverman, S.H., Melling, J., 1985. In vivo evidence that bacteria in urinary tract infection grow under iron-restricted conditions. *Infection and immunity* 48 (1), 35–39.
- Shand, G.H., Anwar, H., Kadurugamuwa, J.A.G.A.T.H., Brown, M.R., Silverman, S.H., Melling, J., 1985. In vivo evidence that bacteria in urinary tract infection grow under iron-restricted conditions. *Infect. Immun.* 48 (1), 35–39.
- Stickler, D., Hughes, G., 1999. Ability of *Proteus mirabilis* to swarm over urethral catheters. *Eur. Clin. Microbiol. Infect.* 18 (3), 206–208.
- Stickler, D.J., Feneley, R.C.L., 2010. The encrustation and blockage of long-term indwelling bladder catheters: a way forward in prevention and control. *Spinal Cord* 48 (11), 784–790.
- Stickler, D.J., 2014. Clinical complications of urinary catheters caused by crystalline biofilms: something needs to be done. *J. Intern. Med.* 276 (2), 120–129.
- Snyder, J.A., Haugen, B.J., Buckles, E.L., Lockett, C.V., Johnson, D.E., Donnenberg, M. S., Mobley, H.L., 2004. Transcriptome of uropathogenic *Escherichia coli* during urinary tract infection. *Infect. Immun.* 72 (11), 6373–6381.
- Tomaras, A.P., Dorsey, C.W., Edelmann, R.E., Actis, L.A., 2003. Attachment to and biofilm formation on abiotic surfaces by *Acinetobacter baumannii*: involvement of a novel chaperone-usher pili assembly system. *Microbiology* 149 (12), 3473–3484.
- Torres, A.G., Redford, P., Welch, R.A., Payne, S.M., 2001. TonB-dependent systems of uropathogenic *Escherichia coli*: aerobactin and heme transport and TonB are required for virulence in the mouse. *Infect. Immun.* 69 (10), 6179–6185.
- Umpiérrez, A., Scavone, P., Romanin, D., Marqués, J.M., Chabalgoity, J.A., Rumbo, M., Zunino, P., 2013. Innate immune responses to *Proteus mirabilis* flagellin in the urinary tract. *Microbes Infect.* 15 (10–11), 688–696.
- Villegas, A., Baronetti, N., Albesa, J., Polifroni, I., Parma, R., Etcheverría, A., Paraje, M., 2013. Relevance of biofilms in the pathogenesis of Shiga-toxin-producing *Escherichia coli* infection. *Sci. World J.* 2013.
- Wazait, H.D., Patel, H.R.H., Veer, V., Kelsey, M., Van Der Meulen, J.H.P., Miller, R.A., Emberton, M., 2003. Catheter-associated urinary tract infections: prevalence of uropathogens and pattern of antimicrobial resistance in a UK hospital (1996–2001). *BJU Int.* 91 (9), 806–809.
- Ye, J., Coulouris, G., Zaretskaya, I., Cutcutache, I., Rozen, S., Madden, T.L., 2012. Primer-BLAST: a tool to design target-specific primers for polymerase chain reaction. *BMC Bioinform.* 13 (1), 1–11.
- Zughaier, S.M., Cornelis, P., 2018. Role of Iron in Bacterial Pathogenesis. *Front. Cell. Infect. Microbiol.* 8, 344.
- Zunino, P., Piccini, C., Legnani-Fajardo, C., 1994. Flagellate and non-flagellate *P. mirabilis* in the development of experimental urinary tract infection. *Microbiol. Pathol.* 16, 379–385.
- Zunino, P., Geymonat, L., Allen, A.G., Legnani-Fajardo, C., Maskell, D.J., 2000. Virulence of a *Proteus mirabilis* ATF isogenic mutant is not impaired in a mouse model of ascending urinary tract infection. *FEMS Immunol. Med. Microbiol.* 29 (2), 137–143.
- Zunino, P., Geymonat, L., Allen, A.G., Preston, A., Sosa, V., Maskell, D.J., 2001. New aspects of the role of MR/P fimbriae in *Proteus mirabilis* urinary tract infection. *FEMS Immunol. Med. Microbiol.* 31 (2), 113–120.
- Zunino, P., Sosa, V., Allen, A.G., Preston, A., Schlapp, G., Maskell, D.J., 2003. *Proteus mirabilis* fimbriae (PMF) are important for both bladder and kidney colonization in mice. *Microbiol* 149 (11), 3231–3237.